

Bayesian Optimization applied for accelerated Virtual Validation of the Autonomous Driving Function

Satyesh Shanker Awasthi, Mohammed Irshadh Ismaaeel Sathyamangalam Imran, Stefano Arrigoni, and Francesco Braghin

Abstract—Rigorous Verification and Validation (V&V) of Autonomous Driving Functions (ADFs) is paramount for ensuring the safety and public acceptance of Autonomous Vehicles (AVs). Current validation relies heavily on simulation to achieve sufficient test coverage within the Operational Design Domain (ODD) of a vehicle, but exhaustively exploring the vast parameter space of possible scenarios is computationally expensive and time-consuming. This work introduces a framework based on Bayesian Optimization (BO) to accelerate the discovery of critical scenarios. We demonstrate the effectiveness of the framework on an Model Predictive Controller (MPC)-based motion planner, showing that it identifies hazardous situations, such as off-road events, using orders of magnitude fewer simulations than brute-force Design of Experiments (DoE) methods. Furthermore, this study investigates the scalability of the framework in higher-dimensional parameter spaces and its ability to identify multiple, distinct critical regions within the ODD of the motion planner used as the case study.

Index Terms—Autonomous vehicles, virtual validation, Bayesian optimization, critical scenarios.

I. INTRODUCTION

A. Why virtual testing and validation is necessary?

Autonomous Vehicles (AVs) promise to revolutionize urban and highway mobility throughout the world. However, the reliability of autonomous driving needs to be proven sufficiently and in little time as possible. On-road testing of Highly Automated Vehicles (HAVs) alone is not sufficient to prove the reliability of Autonomous Driving Systems (ADS), as high-risk driving situations are unlikely to be encountered randomly in real-world miles obtained from naturalistic driving [1], [2]. The space of possible scenarios is effectively infinite, making exhaustive testing infeasible [3]. Moreover, experimental testing might not even be possible in the early V&V phase of ADSs or might be time-consuming and costly [4]. Thus, simulation-based virtual testing is essential for AV safety validation [5], [6].

B. Regulations regarding virtual validation

In recent years, international and regional regulations have recognized the reasons stated above and have initiated accommodating and standardizing, testing and certification of such

vehicles. The World Forum for Harmonization of Vehicle Regulations (WP.29) drafts define “virtual testing” and allow limited use of simulation in type approval [7]. The UNECE-R157 regulation for Automated Lane Keeping Systems (ALKS) already permit certain Software-in-the-Loop (SiL)/Hardware-in-the-Loop (HiL) tests for variant approval [7]. Association for Standardization of Automation and Measuring Systems (ASAM) developed a holistic best practice blueprint to exemplify the diverse testing strategies [8]. In practice, companies like TÜV SÜD advocate a modular validation pipeline by mixing Model-in-the-Loop (MiL), SiL, and HiL tests and systematic scenario catalogs for type approval [9]–[11].

C. Fallbacks of virtual testing

However, even simulation-based testing can be computationally intensive. Brute-force methods like combinatorial testing and Monte Carlo simulation typically require a prohibitively large number of runs for confidence [12], [13]. Advanced uncertainty quantification techniques account for variations in environmental conditions, sensor noise, and behavioral uncertainties, providing robust statistical foundations for safety claims [6], [14]. Sufficient scenario coverage can lead to a significant effort in simulation time and cost and is directly proportional to the number of parameters chosen. To overcome these limitations, generally, two solutions have been explored. The first strategy involves increasing the computational power by implementing massive parallelization of the simulations [15], [16]. The second and more efficient option reduces the number of simulation by using scenario-based frameworks for expediting the scenario search for higher risk scenarios [3], [12]. These tests result in the critical scenarios which could then be retested on the proving grounds for higher fidelity [11]. While testing only the most critical situations is sufficient for ‘type approving’ established systems, a different approach is needed for self-driving systems that are still in development. For these developing systems, safety and performance verification must involve continuous and rapid simulations of both everyday driving situations and high-risk edge cases. These solutions are discussed more in detail in Section II.

D. Contributions

This paper presents a virtual testing and homologation framework in which the critical scenario discovery is formulated as a Bayesian Optimization (BO) problem. This general

validation workflow can be applied to any logical scenario with a given number of input dimensions within a defined Operational Design Domain (ODD). The performance of the framework was further demonstrated in a case study on an autonomous driving motion planner previously developed by the authors [17]. The main contributions of this paper are as follows:

- 1) Bayesian Optimization (BO) framework: We formulate critical scenario discovery as a Bayesian Optimization (BO) problem to find scenario parameters that maximize a safety-violation metric. The framework is agnostic to the scenario specification, allowing any logical scenario with continuous parameters within an ODD to be directly integrated into the Bayesian Optimization loop.
- 2) Application on a developed algorithm: The works present in the literature either focus on early detection of criticality from standard traffic simulations or they are based on naturalistic datasets. To the best knowledge of the authors, this is the first work demonstrating the use of such a framework on a developed ADF.
- 3) Scalability and multiple critical cluster identification: As the number of input dimensions increases, the method consistently identifies failure clusters using one to two orders of magnitude fewer simulations than the equivalent brute-force, full-factorial baseline. Furthermore, the framework successfully locates failures across different types of critical zones that were initially identified through the comprehensive baseline analysis in the applied case study.

E. Arrangement of the paper

The rest of this paper is organized as follows. Section II reviews work related to acceleration of virtual testing techniques. Section III discusses the developed framework in detail, including the optimization problem formulation. Section IV describes the co-simulation methodology as well as the autonomous driving function used to validate the framework. Section V outlines the outcomes and results of the simulations. Finally, Section VI concludes and suggests future work.

II. RELATED WORK

A Verification and Validation (V&V) approach using scenario-based testing for HAVs within a highway ODD was defined in the PEGASUS project [18]. Scenarios within this ODD were classified into functional, logical, and concrete levels to build a comprehensive simulation catalog [19]. This methodology uses extensive simulation to identify critical parameter regions, which are subsequently validated on test tracks [20]. Follow-on projects, such as V&V-Method and SETLevel, have since expanded the ODD to include urban intersection scenarios [21], [22].

Standard random or combinatorial testing is often inefficient at identifying rare failure events. Given that critical scenarios are rare, prioritizing their discovery is essential for reducing testing redundancy. Consequently, recent research has increasingly focused on learning-based and optimization-driven methods to rapidly converge on these safety-critical

scenarios. Several prominent approaches from recent literature are discussed below. One prominent and obvious strategy involves parallel and distributed simulation. In the field of mobility testing, solutions to simulate thousands of scenarios simultaneously, achieving significant improvements in computational speed have been explored. For instance, [23] presents an High-Performance Computing (HPC) pipeline that executes Webots and SUMO simulations in parallel by distributing batch jobs across multiple nodes and instances. In addition, new simulators accelerated by TPUs and GPUs, such as JAX-based engines, are emerging. The Waymax simulator is a differentiable GPU-based traffic simulator capable of simulating up to 128 agents in parallel [15]. These strategies have not been explored in the present work but might be combined with these methods to exploit such simulation toolchains. However, specialized hardware is expensive to purchase and maintain, and keeping up with the latest versions can add significant costs. Furthermore, not all simulation software can utilize hardware acceleration, limiting its benefits and requiring specialized expertise to optimize code for heterogeneous hardware environments.

The emergence of cloud-based simulation platforms represents a shift towards distributed and scalable autonomous vehicle testing. NVIDIA DRIVE Constellation exemplifies the approach through its dual-server architecture, where one server runs DRIVE Sim software to simulate sensor data while a second server contains the DRIVE Pegasus AI car computer running the complete autonomous vehicle software stack [24]. The AVxcelerate Autonomy platform demonstrates the potential of robust, adaptive exploration algorithms optimized for cloud environments, claiming to accelerate sensitivity analyses by a magnitude of 10^3 compared to traditional algorithms [25]. These solutions too could eventually be used in conjunction with the work presented in the paper and have not been explored further. Nevertheless, large-scale cloud usage can become costly over time and moving large simulation datasets to and from the cloud can be slow and expensive.

A more targeted approach uses learning-based techniques to actively generate critical scenarios. Reinforcement Learning (RL) methods, for example, train agents to discover safety violations by modifying scenario parameters like agent trajectories [26]–[28]. DynNPC trains non-player characters to provoke ego-vehicle failures, identifying them 92% faster than static tests [29]. The main objective of these methods is not scenario-coverage but simulating maximum violations achieved during a each test run as quickly as possible after getting trained on a significant amount of episodes. This adversarial approach needs to be re-learned each time the ego vehicle or the underlying Autonomous Driving Function (ADF) changes, rendering this method inefficient for development or homologation processes. RL requires extensive simulation episodes to converge, and shaping reward functions to produce realistic yet critical scenarios is non-trivial. If improperly constrained, these methods can generate physically implausible or irrelevant failure cases.

To mitigate the high computational cost of simulation, [13]

employs surrogate modeling on the whole vehicle system. Since high-fidelity AV simulations are the primary bottleneck, surrogate models built from cheaper, approximate models can accelerate evaluation. However, surrogates are only as good as their training data. Their fidelity can degrade if the operational domain shifts, and they may struggle to capture the highly nonlinear dynamics of complex perception and control systems. Instead of using the surrogates directly for obtaining the results of the simulation, optimization-based testing uses iterative optimization on surrogate models to guide the search toward failure regions efficiently [30], [31]. Heuristic-based optimization methods like genetic algorithms for test parameter optimization for Advanced Driver Assistance Systems (ADAS) testing have also been explored [3], [32], [33]. Bayesian Optimization has also been explored in literature to identify parameterized test conditions that can lead to system failure and to generate new scenarios to be tested in urban scenarios in [34], [35]. A prior work has studied the use of BO with different types of surrogate models to find the worst-case failures in a determined parameter space [36]. This paper leverages Bayesian Optimization to develop a framework for testing and V&V of autonomous vehicles. This framework is then applied to an example autonomous driving function to study the scalability and discovery of multiple critical zones in the ODD of the driving function.

III. PROBLEM FORMULATION : FRAMEWORK

The primary goal of this paper is to introduce a framework for the rapid testing and validation of Autonomous Driving Functions (ADFs), saving significant time and resources during both development and homologation. To achieve this, we have formulated a framework that utilizes Bayesian Optimization (BO) to maximize the probability of simulating critical scenarios. BO is a sample-efficient global optimization method particularly well-suited for problems involving expensive or black-box objective functions, such as high-fidelity vehicle simulations. In the context of scenario-based validation, BO efficiently explores the vast space of simulation parameters to identify critical scenarios—those leading to near-failure or safety-critical behavior—with a minimal number of simulation runs. The process works by modeling an underlying objective, such as a safety metric, with a probabilistic surrogate model like a Gaussian Process. An acquisition function then sequentially selects new test cases by intelligently balancing exploration of uncertain parameter regions and exploitation of areas already known to be critical. This methodology accelerates the discovery of edge cases within the operational design domain (ODD). This approach involves parametric modification of key environmental and behavioral variables, including weather conditions, traffic density, road geometry, and agent behaviors [37]. The critical scenarios are discovered efficiently while maintaining the traceability and repeatability of test conditions.

A. Problem Formulation

The logical scenario (S) is defined as a set of continuous parameters $x \in \mathbb{R}^n$ that describe n number of initial,

Algorithm 1 Bayesian Optimization

Require: Objective function: Criticality metric $f(x)$, search domain: parameter ranges \mathcal{X} , initial dataset: Seed Samples $\mathcal{D}_0 = \{(x_i, f(x_i))\}_{i=1}^{n_0}$, acquisition function $\alpha(x; \mathcal{D})$, maximum iterations or stopping criteria T

Ensure: Approximate maximizer x^*

- 1: Initialize surrogate model (e.g., Gaussian Process) with \mathcal{D}_0
 - 2: **for** $t = n_0 + 1$ to T **do**
 - 3: Select next point $x_t = \arg \max_{x \in \mathcal{X}} \alpha(x; \mathcal{D}_{t-1})$
 - 4: Evaluate objective: $y_t = f(x_t)$
 - 5: Update dataset: $\mathcal{D}_t = \mathcal{D}_{t-1} \cup \{(x_t, y_t)\}$
 - 6: Update surrogate model with \mathcal{D}_t
 - 7: **end for**
 - 8: **return** $x^* = \arg \max_{x_i \in \mathcal{D}_T} f(x_i)$
-

environment, and dynamic parameters with the ODD of the vehicle. Given x , the simulation produces a failure or criticality metric $f(x)$ that quantifies the criticality of the scenario. Thus, the problem of finding the critical scenario reduces to identifying x that maximizes $f(x)$. Since each evaluation of $f(x)$ requires an expensive simulation run, this is cast as a black-box optimization problem.

B. The Optimization framework

Figure 1 illustrates the overall architecture of the proposed simulation acceleration framework using Bayesian Optimization (BO) for critical scenario discovery in autonomous vehicle testing. The process begins with the definition of a logical scenario (S), where the operational design domain (ODD) is parameterized (e.g., ego speed, obstacle speed, initial ego position), $x = [p_1, p_2, \dots, p_n]$. A concrete scenario is instantiated by sampling a specific set of parameters within these ranges. Initial seed samples (S_{seed}) are selected to randomly initialize the BO process as represented by the blue arrow loop. Each sampled scenario is evaluated through a co-simulation environment, which couples a high-fidelity vehicle dynamics simulator and a partial or full ADF implementation. This environment simulates the autonomous driving function in a realistic context, producing vehicle state trajectories and control signals. A criticality metric such as Time to Collision (TTC) or Post Encroachment Time (PET) is computed for each simulation to assess the criticality of the simulation for the given parameter set [38]. Based on the outcomes, a surrogate model is updated and used by an acquisition function to propose the next promising scenario to evaluate as represented by the green arrow loop in Figure 1. The loop continues until a stopping criterion is met, for example, a maximum number of simulations is reached. In this work, the loop terminates either when a decided number of simulations have been completed or until at least one instance in all the critical clusters, identified during baseline simulations, has been found. This architecture ensures that computational resources are focused on discovering high-risk scenarios efficiently.

The algorithmic workflow is presented in Algorithm 1. The description of individual components of the working loop is

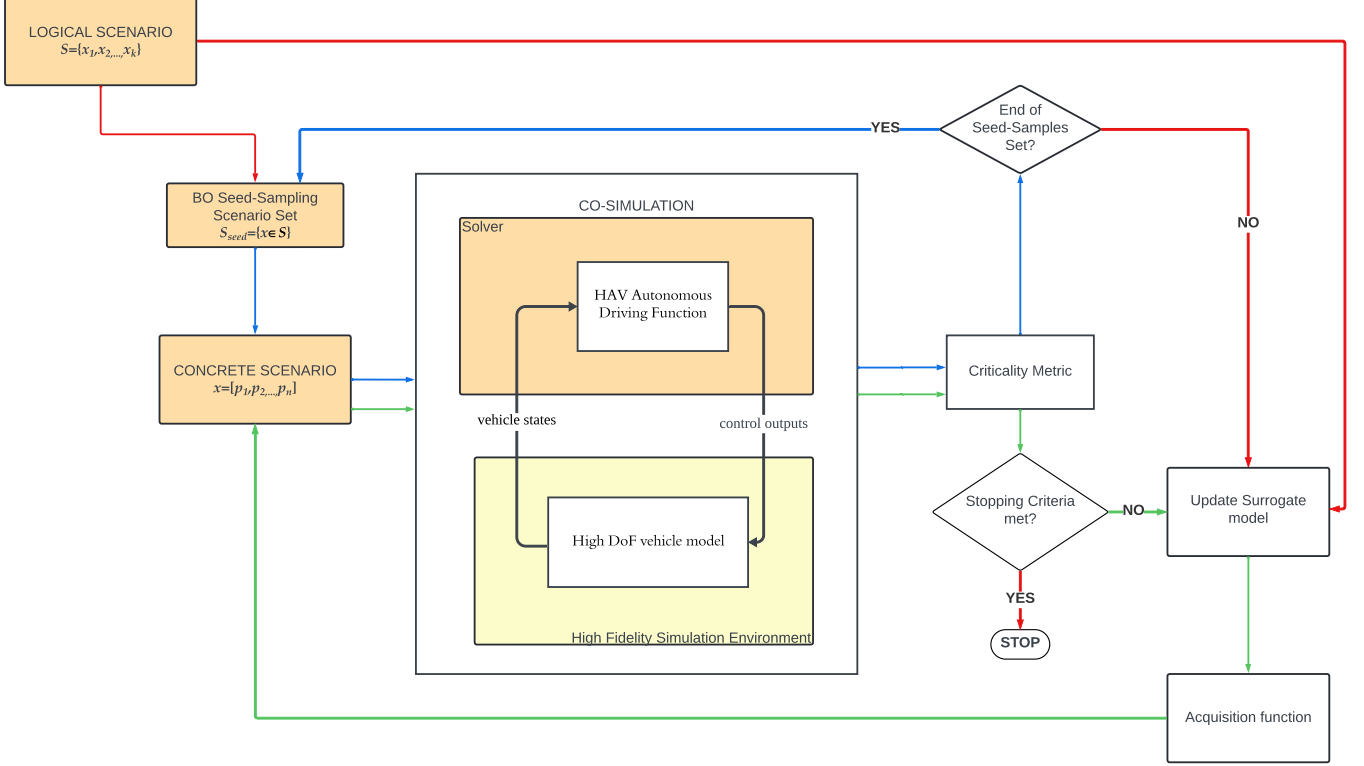


Fig. 1: Layout of feedback loop established between the developed motion planner and the high-fidelity simulation software in the accelerated validation framework loop.

as following:

- 1) *Initialization*: Sample an initial set of scenario parameters $\{x_i\}$ and evaluate the simulator to obtain $\{f(x_i)\}$. The choice of sampling method and number of initial points affects convergence speed and overall performance. There are several methods to choose these initial set of simulations such as: grid sampling, random sampling, sobol sequence and latin hypercube sampling. Any of these methods may be used in this framework but latin hypercube sampling has been used in the case study presented later because it promises better input space coverage [39]. The initial samples increase with the dimensionality of the logical scenario parameters. As a rule of thumb, the seed samples may range from two to five times the number of parameters chosen [40].
- 2) *Surrogate model*: Fit a Gaussian process (GP) regression model to the accumulated data $\{(x_i, f(x_i))\}$. The GP provides a posterior mean and variance over the function $f(x)$. Other probabilistic surrogate models include bayesian neural networks and tree-based random forest. In this work, the underlying objective function $f(x)$, representing the criticality metric in a scenario defined by parameters $x \in \mathbb{R}^n$, is modeled as a Gaussian Process (GP):

$$f(x) \sim \mathcal{GP}(0, k(x, x')), \quad (1)$$

where $k(x, x')$ is the covariance function or kernel encoding assumptions about the smoothness of the func-

tion. It defines the covariance between the values of the function at two different input points, x and x' . The surrogate model is a zero-mean Gaussian Process with a squared exponential kernel given by:

$$k_{SE}(x, x') = \sigma_f^2 \exp\left(-\frac{1}{2}(x - x')^\top \Lambda^{-1}(x - x')\right), \quad (2)$$

where $\Lambda = \text{diag}(\ell_1^2, \ell_2^2, \dots, \ell_d^2)$ is a diagonal matrix of squared length-scales, and σ_f^2 is the signal variance. Hyperparameters of $f(x)$ (length-scales and variance) are learned by maximizing the marginal likelihood. The hyperparameters $\theta = \{\ell_i, \sigma_f^2, \sigma_n^2\}$ are estimated by maximizing the log marginal likelihood:

$$\log p(\mathbf{y} \mid \mathbf{X}, \theta) = -\frac{1}{2} \mathbf{y}^\top K_\theta^{-1} \mathbf{y} - \frac{1}{2} \log |K_\theta| - \frac{n}{2} \log 2\pi, \quad (3)$$

where $K_\theta = K + \sigma_n^2 I$ is the covariance matrix with added observation noise σ_n^2 and \mathbf{y} is the observed data at each x in \mathbf{X} .

The GP surrogate captures the relationship between scenario parameters and the criticality metric. We rely on the GP surrogate to estimate which untested scenarios may be critical. Given training data $\mathcal{D} = \{\mathbf{X}, \mathbf{y}\}$, the predictive distribution at a new input x_* is Gaussian:

$$\mu(x_*) = k_*^\top K^{-1} \mathbf{y}, \quad (4)$$

$$\sigma^2(x_*) = k(x_*, x_*) - k_*^\top K^{-1} k_*, \quad (5)$$

where $k_* = k(\mathbf{X}, x_*)$ is the covariance vector between x_* and the training points.

- 3) *Acquisition*: After the GP posterior has been evaluated, the next input point for the simulation is chosen using an acquisition function, which guides the search by balancing exploration and exploitation. In this work, we use Thompson Sampling, a Bayesian strategy where a random function, $\tilde{f}(x)$, is drawn from the GP posterior. The next point to simulate, x_{next} , is selected by finding the maximizer of this sampled function, as if it were the true objective:

$$x_{\text{next}} = \arg \max_{x \in \mathcal{X}} \tilde{f}(x) \quad (6)$$

where $\mathcal{D} = \{(x_i, y_i)\}_{i=1}^n$ is the current dataset. In Section V, this method is compared to the *Probability of Improvement* acquisition function, which is a utility-based criterion defined as the likelihood that a new candidate point x will improve over the current best observed value y^+ (assuming maximization):

$$\text{PI}(x) = \mathbb{P}(f(x) \geq y^+ + \xi) = \Phi\left(\frac{\mu(x) - y^+ - \xi}{\sigma(x)}\right), \quad (7)$$

where:

- $\mu(x)$ and $\sigma(x)$ are the GP posterior mean and standard deviation,
- $y^+ = \max_{i=1, \dots, n} y_i$ is the best observed value,
- $\xi \geq 0$ is a margin parameter encouraging exploration,
- $\Phi(\cdot)$ is the CDF of the standard normal distribution.

The next point to be simulated, as in the case of Equation 6, when using probability of improvement acquisition function is selected by:

$$x_{\text{next}} = \arg \max_{x \in \mathcal{X}} \text{PI}(x) \quad (8)$$

Other acquisition functions like expected Improvement and Upper Confidence Bound have been tested too but not included in the results presented.

- 4) *Evaluation*: Run the simulator at x_{next} and compute $f(x_{\text{next}})$.
- 5) *Update*: Augment the dataset with $(x_{\text{next}}, f(x_{\text{next}}))$ and go to step 2.

The process repeats until a budget of simulations is exhausted or a convergence criterion is met. BO builds a surrogate for the objective with a GP and uses an acquisition function to decide where to sample.

IV. FRAMEWORK VALIDATION SETUP: METHODOLOGY

In this section, the virtual validation framework is applied to a specific use case: a motion planner for a Highly Automated Vehicle (HAV) operating within an Operational Design Domain (ODD) defined as a straight, two-lane highway

with preceding traffic. It should be noted that the ODD in which this example ADF works has been oversimplified for demonstration purposes. The motion planner follows a straight path and avoids the obstacles that fall into its path by overtaking or following. A detailed overview of the motion-planner formulation is presented in [17]. The ego vehicle starts in the right lane behind the obstacle vehicle. The aim of the study is to validate that the developed framework finds the critical scenarios or failures for the algorithm being tested faster than the baseline methods. The results obtained from the validation framework are compared with the validation results obtained from baseline combinatorial simulations. In addition to the general methodology discussed in Section III, the choice of various components in Figure 1 for this particular application has also been discussed in detail.

To demonstrate the intuition behind the validation method and then the scalability of the parameter space, two sets of parameters have been chosen. Firstly, a set of 3 variable input parameters (3-Degree of Freedom (DoF) simulation) is chosen: $x_{3\text{-DoF}} = [v_{\text{ego}}, v_{\text{lead}}, d_{0,\text{sep}}]$, which consists of ego-vehicle velocity, leading vehicle velocity, and initial distance between the two vehicles as shown in Figure 2a. A deeper investigation is then provided extending the original set with other 3 additional parameters (6-DoF simulations) that are: lateral ego vehicle position along the lane, wind-gust velocity and road friction representing the environmental parameters i.e. $x_{6\text{-DoF}} = [v_{\text{ego}}, v_{\text{lead}}, d_{0,\text{sep}}, x_{0,\text{ego}}, v_{\text{wind}}, \mu_{\text{road}}]$ (Figure 2b). Note that the wind and road parameters are not explicitly considered in the modeling and closed-loop control of the developed motion planner. Therefore, they should act as disturbance factors or modeling errors. The parameter ranges of the logical scenario, S , are enlisted in Table I.

Parameter description	symbol	Unit	range
Ego velocity	v_{ego}	[m/s]	[5,25]
Leading vehicle velocity	v_{lead}	[m/s]	[0,20]
Initial relative distance	$d_{0,\text{sep}}$	[m]	[50,100]
Initial lateral ego position	$x_{0,\text{ego}}$	[m]	[-0.5,0.5]
Wind gust velocity	v_{wind}	[m/s]	[0,25]
Road friction	μ_{road}	[-]	[0.2,0.8]

TABLE I: Parameters and their range for the logical scenario description

We compare the performance of our framework with simulations performed using full factorial combinatorial testing. For the baseline simulations, only the blue arrow loop of Figure 1 is followed where the seed sample set, S_{seed} is a combination of discretized values considered parameter ranges included in the logical scenario, covering the parameter space uniformly. Instead, for the BO framework, the seed sample set is chosen based on the number of parameters involved according to the research in [40]. We use the rule of thumb of 5x seed simulation runs for training the surrogate model. Additional tests of the green-arrow Bayesian optimization

loop in Figure 1 are then performed until the stopping criteria are met.

The co-simulation environment couples a model-predictive controller in MATLAB/Simulink with the IPG CarMaker vehicle simulator for closed-loop behavior [41], [42]. In Simulink, the ego vehicle executes a rule-defined motion planner based on an *adaptive MPC* framework, formulated via CasADi and solved by *acados* [43], [44]. Following the work [17] and [45], this planner embeds high-level driving rules, which include overtaking, following or stopping, directly within the MPC by adapting both the cost-function weights and Control Barrier Function (CBF) parameters (γ and D_{OV}) based on the scenario detected. The weights remain unchanged from the work presented in [45] and the correct sets of weights are automatically chosen during each simulation run. For instance, during overtaking, lateral deviation is penalized less while velocity tracking is emphasized, paired with a tight safety margin; conversely, during following or stopping, the longitudinal error is weighted more heavily and the CBF parameters are adjusted to prioritize lane adherence or complete stop. The obstacle vehicle follows a simple velocity profile. The Simulink MPC outputs acceleration or brake and steering commands to the simulator, which models realistic vehicle dynamics. This closed-loop setup captures how control decisions (e.g., steering to avoid the obstacle) interact with the vehicle physics. For each concrete scenario x , the co-simulation runs for a fixed duration or until an off-road event. Note that no collisions occur because of the inherent modeling of the MPC where CBF is a hard constraint. Two failure modes exist. The first one includes off-road events due to runtime solver failure, in which the solver initially finds a solution but eventually fails due to the constraints present. The second failure mode is the *a priori* solver infeasibility, failing to find any valid solution to the simulation requested.

Although standard criticality metrics such as Time-to-Collision (TTC) or Post-Encroachment Time (PET) could

serve as the objective function [38], this work uses two more direct metrics: the maximum lateral displacement of the ego vehicle and the solver infeasibility status. This choice is motivated by the two failure modes under consideration as discussed above. Off-road events can occur when the ego vehicle, influenced by the Control Barrier Function (CBF) of the leading vehicle, overshoots the road boundary. Minimizing lateral displacement, therefore, directly addresses this specific failure mechanism. The solver status is instead a discrete metric that indicates whether the infeasibility of the solution is due to the initial conditions (the scenarios is unable to be handled by the solver) or eventual runtime infeasibility due to the MPC constraints.

The iteration of the Bayesian Optimization framework simulations terminate when at least one instance in each of the critical clusters identified in the baseline simulations are identified. The identification of clusters for the given case study is discussed more in detail in Section V. However, an upper bound for the number of simulations to be performed is set at one order of simulations less than the ones presented in the baseline case. This has been done to analyze the performance of the validation framework as the framework would not be beneficial if the simulations required are in the same order as those of the baseline case. Different combinations of the acquisition functions and Hence this paper also benchmarks for the stopping criteria by comparing the baseline simulations with the ones executed with the BO framework. The statistical analysis of the results obtained using different combinations of acquisition functions and criticality metrics are present in Section V.

V. CASE STUDY RESULTS

A. Case A: 3-DoF simulations

To establish a baseline for comparison, an exhaustive full-factorial Design of Experiments (DoE) was conducted across a discretized, three-degree-of-freedom (3-DOF) parameter space. This 3-DOF case was chosen because it represents the maximum dimensionality in which the results can be completely visualized, thereby providing an intuitive understanding

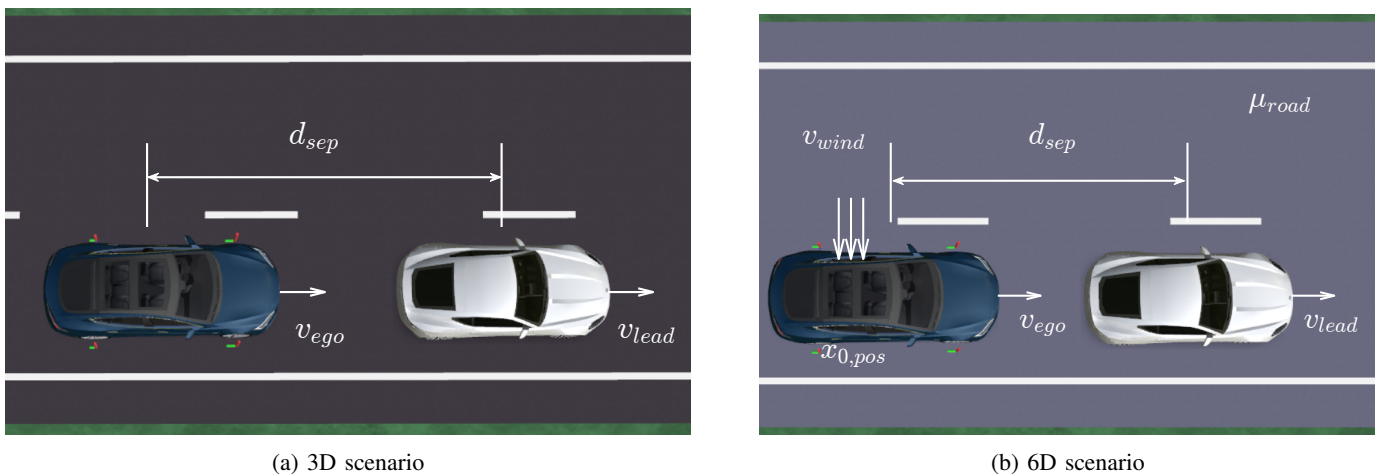


Fig. 2: A scene from the logical scenario being tested and three variable parameters of the logical scenario

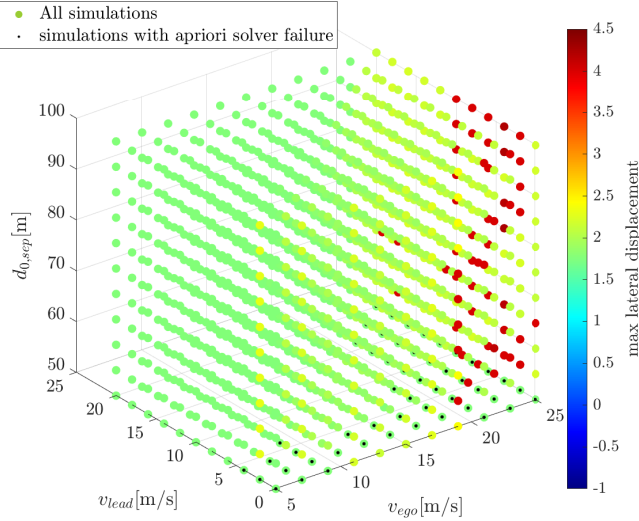


Fig. 3: Baseline simulation results of the 3-DOF simulations. The parameter sweep covers ego speed, obstacle speed, and initial distance between them. Off-road scenarios are marked in red, representing critical failures.

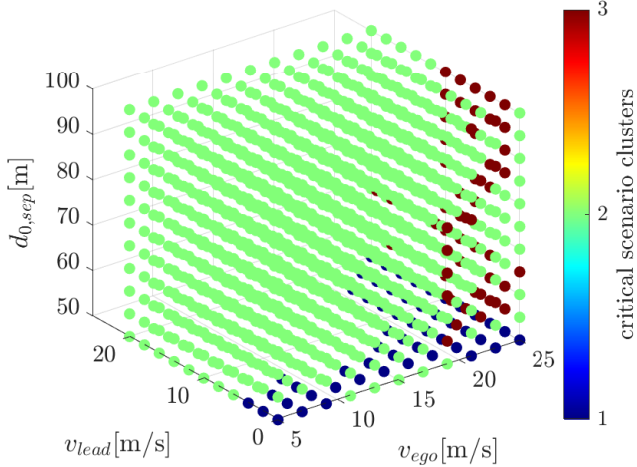


Fig. 4: The two principal clusters identified by the two criticality metrics used: A continuous metric-max lateral displacement of the AV and a discrete metric-MPC solver status

of the methodology. The scenario parameters include the ego vehicle’s speed (ranging from 5 to 25 m/s in 2 m/s increments), the leading vehicle’s speed (from 0 to 20 m/s in 2 m/s increments), and the initial spacing (from 50 to 100 m in 5 m increments). This discretization results in $11 \times 11 \times 11 = 1331$ unique scenarios.

For each configuration, a co-simulation evaluates the ego vehicle’s trajectory under MPC control. As discussed in Section IV, the motion planner can exhibit two types of failures; consequently, this case study uses two corresponding criticality metrics: one continuous and one discrete. The continuous metric is the maximum lateral displacement of the vehicle from the centerline, with a failure threshold set

to 3.5 m to match the lane width. The discrete metric is the solver’s infeasibility status, indicating the operational limits of the controller, where a status of 4 denotes a null simulation (due to *a priori* infeasibility) and 0 represents a successfully executed simulation. A single value for all the criticality metrics considered is obtained from each simulation run.

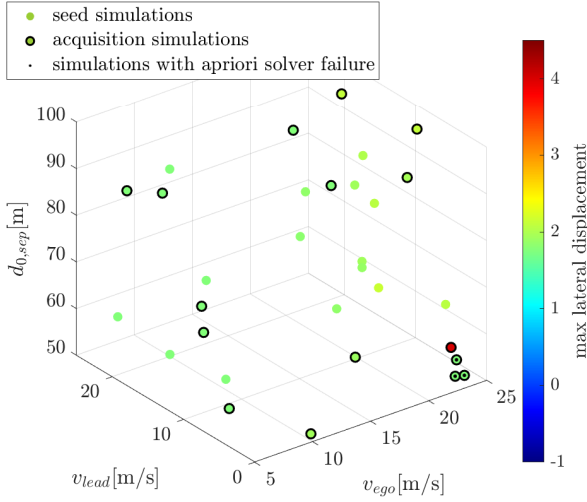
Figure 3 summarizes these results, highlighting the value of the continuous criticality metric—the absolute maximum lateral displacement from the centerline. As shown in the figure, the most extreme cases correspond to combinations of high relative speed and small initial spacing between the vehicles. It is also evident that failures (off-road events) occur in the region where this metric exceeds the 3.5 m lane-width threshold. Simulations resulting in *a priori* failure due to initial condition infeasibility are marked with a dot inside the simulation marker in Figure 3. In these cases, since no trajectory data is produced, the maximum lateral displacement metric equals the centerline of the lane, that is 1.75 m, which is the initial starting position of the ego vehicle. This comprehensive dataset serves as the ground truth for validating the sample efficiency of the Bayesian optimization approach, which seeks to discover these same critical regions using significantly fewer simulations.

To identify the critical zones in the logical scenario space, clustering of the criticality metrics resulting from the baseline simulations is performed. Density-Based Spatial Clustering of Applications with Noise (DBSCAN) algorithm was used to cluster the results into groups of varying sizes [46]. This clustering algorithm was chosen so that it could be applied to any n -dimensional space and hence it could account for multiple criticality metrics as input. Figure 4 shows the three clusters found using the criticality metric vector as input to the algorithm. Two of these three clusters are critical ones pertaining to the ego crossing the road bounds (Cluster 3) and *a priori* solver failure (Cluster 1). The third and the biggest cluster (Cluster 2) is of the simulations where the controller successfully performs the necessary manoeuvre. The size of the clusters is reported in Table II.

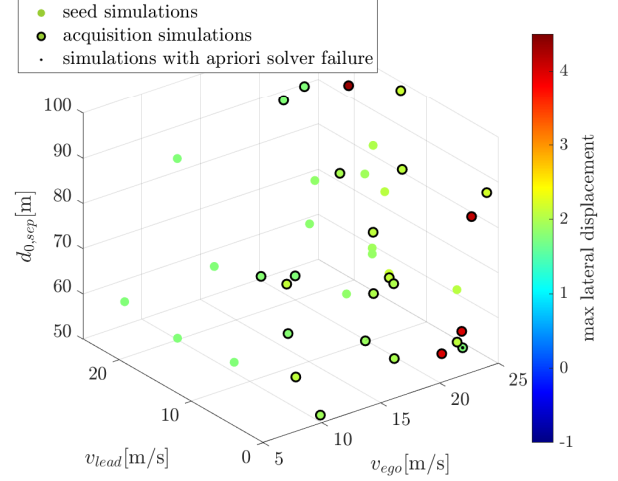
Simulation set	Cluster 1	Cluster 2	Cluster 3	Total simulations
3-DoF	52	1223	56	1331
6-DoF	720	12906	6174	19800

TABLE II: Sizes of the clusters found in the baseline simulations. Clusters 1 and 3 are the critical clusters related to off-road events and *a priori* solver failure respectively.

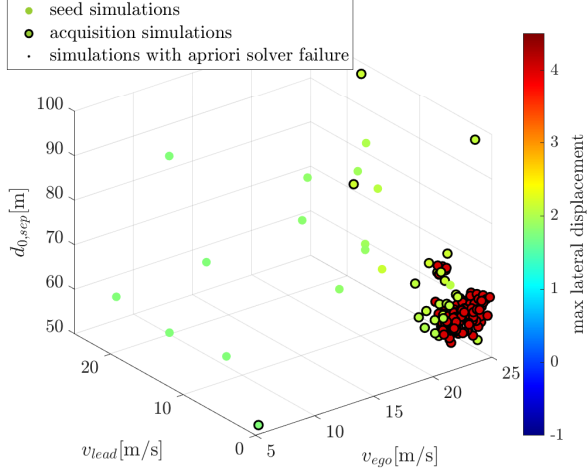
The validation of the Bayesian Optimization (BO) framework aims to confirm its ability to rapidly explore and identify critical scenarios. While a single detected failure would typically invalidate the system for a fixed Operational Design Domain (ODD), one of the objectives of this work is to analyze the capability of the framework to detect multiple, distinct failures or critical zones. To achieve this objective, multiple acquisition functions as previously mentioned in Section III have been thoroughly tested. The choice of acquisition function can balance the exploration with exploitation and can prevent the



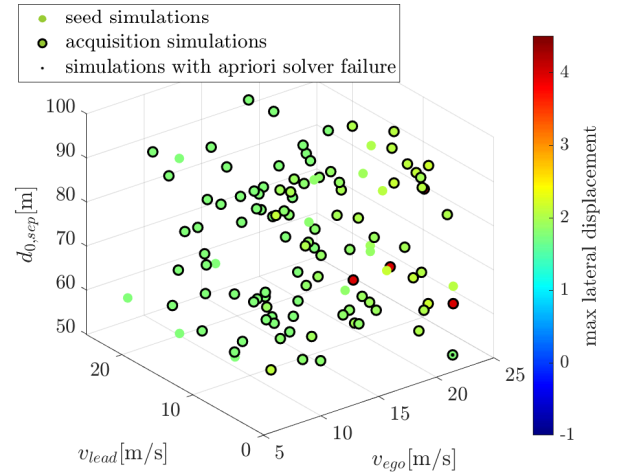
(a) Simulation A: Thompson Sampling and MPC Solver status



(b) Simulation B: Thompson Sampling and max lateral displacement



(c) Simulation C: Probability of Improvement and max lateral displacement



(d) Simulation D: Probability of Improvement and MPC Solver status

Fig. 5: One complete run each of the 3 simulation categories with the same seed sample. The seed runs and the acquisition runs are distinguished by the marker edge: (a) discrete metric triggers exploration of the parameter space, (b) continuous metric leads to exploitation of overtake scenario parameters (c) exploitation of local minimum, only one cluster identified (d) exploration of the full logical scenario space until both critical types are found.

optimization getting stuck in a local minimum. Results including two of these acquisition functions, Thompson Sampling and Probability of Improvement (PI), in the test runs have been presented henceforth. Thompson Sampling naturally balances exploration and exploitation whereas PI tends to be greedy and more exploitative..

Four sets (A, B, C and D) of 10 simulations each were performed to study the behaviour of using different types of criticality metrics (continuous vs discrete) to form the surrogate model and different acquisition functions (balanced vs greedy) for evaluating the next concrete scenario simulation parameter values. One instance each of these 4 sets with the same seed samples for training the surrogate model is shown in Figure 5. Simulation sets A and B both use Thompson Sampling as the acquisition function whereas C and D use Probability of Improvement (PI) function. Furthermore, A and

D use the discrete criticality metric (solver status) while B and C use the continuous metric (maximum lateral displacement of the ego). It is apparent from Figure 5a that since the surrogate is trained on the discrete metric, the acquisition simulations are based on pure exploration of the parameter ranges until the critical cases are found in the lower right corner whereas in Figure 5b the acquisition simulations are biased towards the higher velocity difference between the two vehicles where the overtaking and hence the higher lateral displacement occurs. In Figure 5c, the exploitation is more prevalent than exploration and once the failure is detected the new acquisition points remain close by. From Figure 5d, exploration characteristic of the PI acquisition function is visualized since using a discrete metric does not add any new information to the surrogate model until the critical zone is found by searching in uncertain areas of the parameter space. Furthermore, in the plotted case

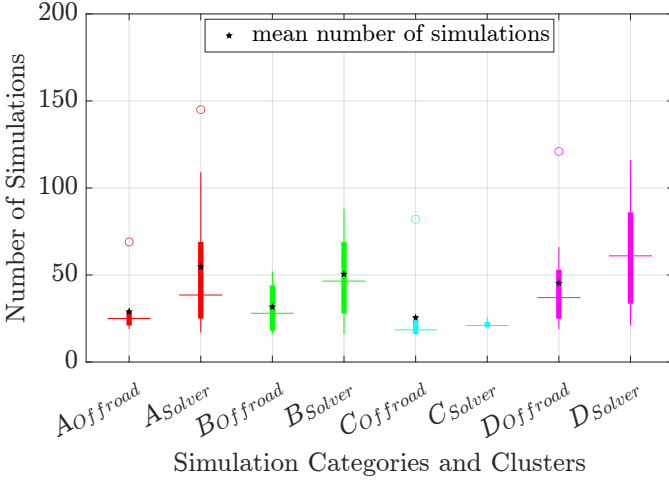


Fig. 6: 4 categories of 10 sets of simulations. A: Criticality metric is solver status(discrete) and the acquisition function is Thompson sampling. B: Criticality metric is max lateral displacement of ego(continuous)and the acquisition function is Thompson sampling. C: Criticality metric is max lateral displacement of ego(continuous)and the acquisition function is Probability of Improvement. D: Criticality metric is solver status(discrete) and the acquisition function is Probability of Improvement.

of simulations C, critical scenarios pertaining to Cluster 1 were not found while in A, B, and D, instances in both clusters were successfully identified.

The box plots of the results that compare these simulations is presented in Figure 6. The plots present a statistical analysis of the number of simulations performed before the first detection of critical scenario in each identified critical cluster starting with different seed simulations. This difference occurs due to the stochastic Latin Hypercube Sampling of the initial simulations. The numbers include the initial seed simulation runs, which is equal to 15 in this case. The upper bound for the framework iterations was set at 150 simulations. It can be seen from the box plot that the mean and median number of simulations required in each case to find the first critical scenario of each cluster is less than 100 simulations which is one order less than the baseline simulations. However, Simulation C and D, using the PI acquisition function were unable to find both critical zones 5 and 2 times out of 10 respectively, hence the mean values in this case haven't been included. It can also be observed that the discovery of the offroad events' cluster has less variance and gets detected earlier in average when compared to the solver-failure cluster. The median simulations required to find the solver-failure cluster is always greater but always remain in the same order less than the baseline simulations. Thus, from Figure 5 and Figure 6 it can be seen that continuous metrics drive the discovery of critical points by creating meaningful surrogate model whereas discrete metrics rely on the exploration of the scenario space by the acquisition function to do so. If exploitation-favored configurations of acquisition functions like PI are used with other metrics (the case of Simulation

C), it's difficult to discover critical instances pertaining to the discrete metric using this framework. However, using acquisition functions that are inherently balanced between exploration and exploitation like Thompson Sampling may solve this issue although requiring more simulations in average. The combination of using Thompson Sampling with a continuous metric (Simulation B) is the only one without outliers.

B. Case B: 6-DoF simulations

To evaluate the framework's scalability, the parameter space was expanded to six dimensions by adding three new parameters, with ranges as defined in Section IV. These new parameters are the ego vehicle's initial lateral offset from the centerline, the lateral wind gust velocity, and the road friction coefficient. The wind velocity was varied up to 25 m/s, corresponding to a 'whole gale' on the Beaufort scale (Force 10). The road friction coefficient, μ , ranged from 0.2 (representing icy conditions) to 0.8 (representing dry asphalt). In total, $5 \times 5 \times 11 \times 3 \times 6 \times 4 = 19,800$ baseline simulations were performed across the expanded parameter space as presented in Table I. A representative subset of these results, for a constant wind velocity of 15 m/s, is shown in Figure 7. The critical scenarios are marked in red, representing crossing of the road limits. The *a priori* solver failure simulations are represented as dark blue dots by assigning them a value of -1 for ease of visualization only. It could be seen from the subplots that wind and low road frictions have a destabilizing effect on the vehicle and the aggressive motion-planner commands at high speed overtake maneuvers result in the vehicle exiting the road boundaries almost throughout the set ODD. A decrease in the number of critical scenarios from the leftmost to the rightmost subplots of the image can also be observed. This is due to the increase in road friction parameters as reported in the figure. The relative starting position in the given range has little effect on the criticality of the simulation as the subplots remain almost the same from the top to the bottom. This 6-DOF case involves an order of magnitude more simulations than the 3-DOF analysis presented previously. Using the DBSCAN clustering algorithm, two distinct critical clusters were again identified, corresponding to *a priori* solver failure and off-road events, consistent with the findings in Section V-A. The sizes of these clusters are detailed in Table II. The objective remains to evaluate the BO framework's capability to efficiently detect these distinct critical zones.

To assess the framework's performance, two simulation sets (E and F) were conducted, with results summarized in Figure 8. For both sets, the initial seed sample size was set to five times the parameter space dimension, amounting to 30 scenarios. To ensure a valid comparison, these 30 initial simulations are included in the total counts, and the same seed samples were used for both Set E and Set F.

Simulation Set E is analogous to the best-performing approach from the 3-DOF case, where the continuous metric (maximum lateral displacement) was used to train the surrogate model, and Thompson Sampling selected subsequent test cases. This approach proved highly efficient at discovering the off-road events, likely because the large size of this cluster

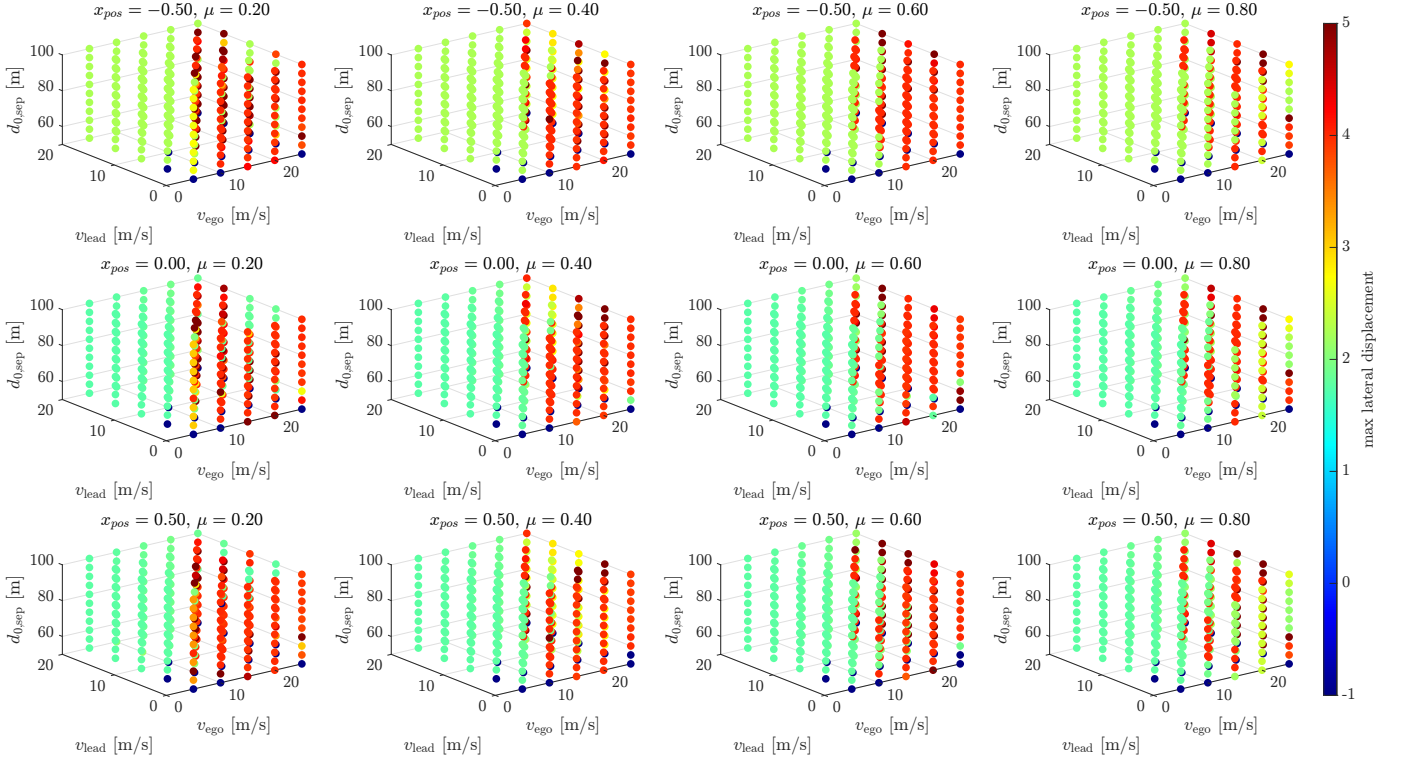


Fig. 7: Simulations performed for wind gust velocity = 15 m/s. each subplot represents the 3-D equivalent simulations for each discrete value combination of the road friction coefficient and starting x position along the road.

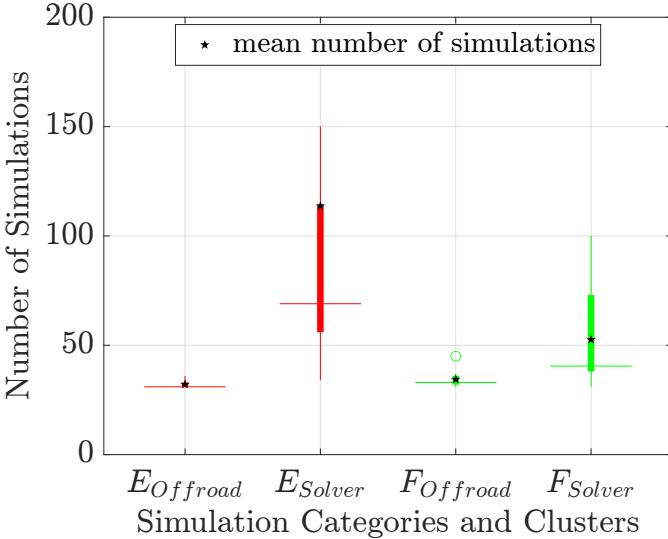


Fig. 8: 2 categories of 10 sets of simulations. A: Criticality metric is max lateral displacement of ego(continuous) and the acquisition function is Thompson sampling. B: Alternate criticality metrics are used to form the surrogate: max lateral displacement of ego(continuous) and the solver status(discrete). The acquisition function is Thompson sampling.

increased the probability of finding a critical point within the initial seed set. However, this single-metric strategy struggled to identify the smaller solver-failure cluster, exhibiting high variance and requiring significantly more simulations. The

mean number of simulations for this task was skewed by an outlier run of 472 simulations (not shown in the figure), highlighting the potential unreliability of relying on a single metric to find all failure types.

To address this limitation, a hybrid strategy was tested in Set F. This approach alternates between the two criticality metrics obtained as the results of simulations to train the surrogate model in subsequent iterations. As shown in Figure 8, the hybrid strategy of Set F yields a superior and more balanced performance. Training the surrogate on the discrete solver-failure metric promotes broader exploration of the parameter space, which significantly reduces the mean, median, and variance of the simulations required to identify the smaller, harder-to-find cluster. The framework's overall efficiency remains comparable to the 3-DOF case, indicating that it is highly scalable. In this 6-DOF study, the proposed method is two orders of magnitude more efficient than the baseline combinatorial testing.

VI. CONCLUSION AND FUTURE WORK

This paper introduces a framework for the accelerated virtual validation of an Autonomous Driving Function (ADF). The framework combines Scenario-Based Testing (SBT) with Bayesian Optimization to efficiently discover critical scenarios by iteratively fitting a Gaussian Process surrogate model to simulation outcomes. New test cases are selected using acquisition functions that maximize a predicted failure metric. This approach identifies safety violations, such as off-road events and solver failures, with orders of magnitude fewer simulations than brute-force methods. A key advantage of this work is its

flexible, model-agnostic workflow, which can handle diverse logical scenario definitions and high-dimensional parameter spaces within a given ODD.

The framework's effectiveness was demonstrated through a use case involving a Model Predictive Controller (MPC)-based motion planner operating on a two-lane highway with preceding traffic. A co-simulation platform integrating MATLAB/Simulink, the acados MPC solver, and IPG CarMaker provided a realistic testbed. The results show that the framework successfully identifies distinct critical clusters that were previously found via baseline full-factorial testing. The method performs most robustly when the surrogate model is developed with continuous criticality metrics and when using acquisition functions, such as Thompson Sampling, that naturally balance exploration and exploitation. Furthermore, a hybrid strategy that alternates between different criticality metrics to train the surrogate model was explored and found to be highly effective.

To demonstrate scalability, the framework was applied to the same Autonomous Driving Function (ADF) while doubling the parameter space from three to six variables. The approach proved to be scalable, detecting the critical clusters up to two orders of magnitude more efficiently than the baseline ground-truth simulations. This framework, therefore, shows significant promise for expediting the development and homologation processes of autonomous driving functions when integrated into virtual testing toolchains.

Future work will focus on applying this framework to more complex, multi-agent scenarios in urban environments and integrating perception and localization modules into the simulation loop. Further extensions will explore multi-fidelity modeling and multi-objective optimization to simultaneously find failures under different criteria. Ultimately, this line of research aims to provide rigorous and scalable tools for AV safety assurance by focusing testing efforts on the most challenging scenarios.

REFERENCES

- [1] N. Kalra and S. M. Paddock, "Driving to safety: How many miles of driving would it take to demonstrate autonomous vehicle reliability?" *Transportation Research Part A: Policy and Practice*, vol. 94, pp. 182–193, 2016. [Online]. Available: <https://www.sciencedirect.com/science/article/pii/S0965856416302129>
- [2] L. Vater, M. Sonntag, J. Hiller, P. Schaudt, and L. Eckstein, "A systematic approach towards the definition of the terms edge case and corner case for automated driving," in *2023 3rd International Conference on Electrical, Computer, Communications and Mechatronics Engineering (ICECCME)*, 2023, pp. 1–6.
- [3] X. Zhang, J. Tao, K. Tan, M. Törngren, J. M. G. Sánchez, M. R. Ramli, X. Tao, M. Gyllenhammar, F. Wotawa, N. Mohan, M. Nica, and H. Felbinger, "Finding critical scenarios for automated driving systems: A systematic mapping study," *IEEE Trans. Softw. Eng.*, vol. 49, no. 3, p. 991–1026, 2023. [Online]. Available: <https://doi.org/10.1109/TSE.2022.3170122>
- [4] P. Koopman and M. Wagner, "Challenges in autonomous vehicle testing and validation," *SAE Int. J. Trans. Safety*, 2016.
- [5] R. Donà and B. Ciuffo, "Virtual testing of automated driving systems. a survey on validation methods," *IEEE Access*, vol. 10, pp. 24 349–24 367, 2022.
- [6] X. Zhao, R. Aghazadeh-Chakherlou, C.-H. Cheng, P. Popov, and L. Strigini, "On the need for a statistical foundation in scenario-based testing of autonomous vehicles," 2025. [Online]. Available: <https://arxiv.org/abs/2505.02274>
- [7] United Nations Economic Commission for Europe, "Addendum 156 – un regulation no. 157 uniform provisions concerning the approval of vehicles with regards to automated lane keeping system," 2021, accessed: 2024-06-10. [Online]. Available: <https://unece.org/transport/documents/2021/03/standards/un-regulation-no-157-automated-lane-keeping-systems-alks>
- [8] A. for Standardization of Automation and M. Systems, *Evolving Landscapes Of Collaborative Testing For Adas & Ad*. ASAM e.V., 2022.
- [9] S. Riedmaier, J. Nesensohn, C. Gutenkunst, B. Schick, T. Düser, and H. Abdellatif, "Validation of x-in-the-loop approaches for virtual homologation of automated driving functions," in *11. Grazer Symposium Virtual Vehicle(GSVF) Graz*, 15./16.05. 2018, 2018.
- [10] X. Cao, H. Chen, S. Y. Gelbal, B. Aksun-Guvenc, and L. Guvenc, "Vehicle-in-virtual-environment (vve) method for autonomous driving system development, evaluation and demonstration," *Sensors*, vol. 23, no. 11, 2023. [Online]. Available: <https://www.mdpi.com/1424-8220/23/11/5088>
- [11] Z. Fei, M. Andersson, and A. Tingberg, "Correlation of software-in-the-loop simulation with physical testing for autonomous driving," 2024. [Online]. Available: <https://arxiv.org/abs/2406.03040>
- [12] Z. Zhong, Y. Tang, Y. Zhou, V. de Oliveira Neves, Y. Liu, and B. Ray, "A survey on scenario-based testing for automated driving systems in high-fidelity simulation," 2021. [Online]. Available: <https://arxiv.org/abs/2112.00964>
- [13] K. Joshi, C. Hsieh, S. Mitra, and S. Misailovic, "Gas: Generating fast & accurate surrogate models for simulations of autonomous vehicle systems," in *2024 IEEE 35th International Symposium on Software Reliability Engineering (ISSRE)*, 2024, pp. 260–271.
- [14] A. Best, S. Narang, L. Pasqualin, D. Barber, and D. Manocha, "Autonovi-sim: Autonomous vehicle simulation platform with weather, sensing, and traffic control," in *2018 IEEE/CVF Conference on Computer Vision and Pattern Recognition Workshops (CVPRW)*, 2018, pp. 1161–11618.
- [15] C. Gulino, J. Fu, W. Luo, G. Tucker, E. Bronstein, Y. Lu, J. Harb, X. Pan, Y. Wang, X. Chen, J. D. Co-Reyes, R. Agarwal, R. Roelofs, Y. Lu, N. Montali, P. Mougin, Z. Yang, B. White, A. Faust, R. McAllister, D. Anguelov, and B. Sapp, "Waymax: An accelerated, data-driven simulator for large-scale autonomous driving research," 2023. [Online]. Available: <https://arxiv.org/abs/2310.08710>
- [16] F. Indaheng, E. Kim, K. Viswanadha, J. Shenoy, J. Kim, D. J. Fremont, and S. A. Seshia, "A scenario-based platform for testing autonomous vehicle behavior prediction models in simulation," 2021. [Online]. Available: <https://arxiv.org/abs/2110.14870>
- [17] M. I. I. Sathyamangalam Imran, S. S. Awasthi, M. Khayyat, S. Arrigoni, and F. Braghin, "A rule-defined adaptive mpc based motion planner for autonomous driving applications," in *16th International Symposium on Advanced Vehicle Control*. Cham: Springer Nature Switzerland, 2024, pp. 540–549.
- [18] J. Bock, R. Krajewski, L. Eckstein, J. Klimke, J. Sauerbier, and A. Zlocki, "Data basis for scenario-based validation of had on highways," in *27th Aachen colloquium automobile and engine technology*, 2018, pp. 8–10.
- [19] H. Weber, J. Bock, J. Klimke, C. Roesener, J. Hiller, R. Krajewski, A. Zlocki, and L. E. and, "A framework for definition of logical scenarios for safety assurance of automated driving," *Traffic Injury Prevention*, vol. 20, no. sup1, pp. S65–S70, 2019.
- [20] PEGASUS Consortium, "Pegasus—first steps for the safe introduction of automated driving," in *Verification and Validation of Automated Driving Functions*, 2019, project funded by the German Federal Ministry for Economic Affairs and Energy (BMWi); defines scenario-based testing methods for automated driving functions.
- [21] Fraunhofer IESE et al., "Verification & Validation Methods (VVM) for Automated Vehicles," Project page, Fraunhofer IESE / ASAM, 2019–2023, german Federal Ministry-funded extension of PEGASUS scenario-based validation to SAE L4/L5 urban use cases. [Online]. Available: <https://www.vvm-projekt.de/>
- [22] Fraunhofer LBF and partners, "SET Level: Safety for the autonomous mobility of the future," Fraunhofer LBF project page, 2022, develops flexible simulation platforms for VDA L4/L5 automated driving validation. [Online]. Available: <https://www.lbf.fraunhofer.de/en/project/setlevel-safety-autonomous-mobility.html>
- [23] M. Franchi, R. Kahn, M. Chowdhury, S. Khan, K. Kennedy, L. Ngo, and A. Apon, "Webots.hpc: A parallel simulation pipeline for autonomous vehicles," in *Practice and Experience in Advanced Research Computing 2022: Revolutionary: Computing, Connections, You*, ser. PEARC '22. New York, NY, USA: Association for Computing Machinery, 2022. [Online]. Available: <https://doi.org/10.1145/3491418.3535133>

- [24] H. Martinez, "NVIDIA Introduces DRIVE Constellation Simulation System to Safely Drive Autonomous Vehicles Billions of Miles in Virtual Reality," NVIDIA Newsroom, Mar 2018, [Online]. Available: <https://nvidianews.nvidia.com/news/nvidia-introduces-drive-constellation-simulation-system-to-safely-drive-autonomous-vehicles-billions-of-miles-in-virtual-reality>, Accessed on: Jul. 3, 2025.
- [25] Ansys, Inc., "Ansys AVxcelerate Autonomy: End-to-end simulation platform for autonomous vehicle validation," Product overview / press release, December 19, 2023, accessed: 2025-06-25, [Online]. Available: <https://www.ansys.com/products/av-simulation/ansys-avxcelerate-autonomy>
- [26] J. Wu, C. Lu, A. Arrieta, and S. Ali, "Multi-objective reinforcement learning for critical scenario generation of autonomous vehicles," 2025, [Online]. Available: <https://arxiv.org/abs/2502.15792>
- [27] S. Feng, H. Sun, X. Yan, H. Zhu, Z. Zou, S. Shen, and H. X. Liu, "Dense reinforcement learning for safety validation of autonomous vehicles," *Nature*, vol. 615, no. 7953, pp. 620–627, 2023.
- [28] H. Liu, L. Zhang, S. K. Sastry Hari, and J. Zhao, "Safety-critical scenario generation via reinforcement learning based editing," in *2024 IEEE International Conference on Robotics and Automation (ICRA)*, 2024, pp. 14 405–14 412.
- [29] Y. Lu, Y. Tian, D. Wang, B. Chen, and X. Peng, "Dynnp: Finding more violations induced by ads in simulation testing through dynamic npc behavior generation," 2025, [Online]. Available: <https://arxiv.org/abs/2411.19567>
- [30] H. Beglerovic, M. Stolz, and M. Horn, "Testing of autonomous vehicles using surrogate models and stochastic optimization," in *2017 IEEE 20th International Conference on Intelligent Transportation Systems (ITSC)*, 2017, pp. 1–6.
- [31] J. Mullins and S. Mahadevan, "Variable-fidelity model selection for stochastic simulation," *Reliability Engineering & System Safety*, vol. 131, pp. 40–52, 2014, [Online]. Available: <https://www.sciencedirect.com/science/article/pii/S0951832014001331>
- [32] F. Klück, M. Zimmermann, F. Wotawa, and M. Nica, "Genetic algorithm-based test parameter optimization for adas system testing," in *2019 IEEE 19th International Conference on Software Quality, Reliability and Security (QRS)*, 2019, pp. 418–425.
- [33] R. Ben Abdesslem, S. Nejati, L. C. Briand, and T. Stifter, "Testing vision-based control systems using learnable evolutionary algorithms," in *2018 IEEE/ACM 40th International Conference on Software Engineering (ICSE)*, 2018, pp. 1016–1026.
- [34] B. Gangopadhyay, S. Khastgir, S. Dey, P. Dasgupta, G. Montana, and P. Jennings, "Identification of test cases for automated driving systems using bayesian optimization," in *2019 IEEE Intelligent Transportation Systems Conference (ITSC)*, 2019, pp. 1961–1967.
- [35] B. Schütt, M. Heinrich, S. Marahrens, J. M. Zöllner, and E. Sax, "An application of scenario exploration to find new scenarios for the development and testing of automated driving systems in urban scenarios," in *Proceedings of the 8th International Conference on Vehicle Technology and Intelligent Transport Systems - VEHITS, INSTICC*. SciTePress, 2022, pp. 338–345.
- [36] Y. Huang, J. Sun, and Y. Tian, "A bayesian optimization method for finding the worst-case scenarios of autonomous vehicles," *IEEE Transactions on Intelligent Transportation Systems*, vol. 26, no. 1, pp. 529–543, 2025.
- [37] H. Weber, J. Bock, J. Klimke, C. Roesener, J. Hiller, R. Krajewski, A. Zlocki, and L. Eckstein, "A framework for definition of logical scenarios for safety assurance of automated driving," *Traffic injury prevention*, vol. 20, no. sup1, pp. S65–S70, 2019.
- [38] L. Westhofen, C. Neurohr, T. Koopmann, M. Butz, B. Schütt, F. Utesch, B. Neurohr, C. Gutenkunst, and E. Böde, "Criticality metrics for automated driving: A review and suitability analysis of the state of the art," *Archives of Computational Methods in Engineering*, vol. 30, no. 1, pp. 1–35, 2023.
- [39] R. L. Iman, *Latin Hypercube Sampling*. John Wiley & Sons, Ltd, 2008, [Online]. Available: <https://onlinelibrary.wiley.com/doi/abs/10.1002/9780470061596.risk0299>
- [40] P. I. Frazier, "A tutorial on bayesian optimization," 2018, [Online]. Available: <https://arxiv.org/abs/1807.02811>
- [41] T. M. Inc., "Matlab version: 9.8.0 (r2020b)," Natick, Massachusetts, United States, 2020, [Online]. Available: <https://www.mathworks.com>
- [42] IPG Automotive GmbH, "Carmaker," Karlsruhe, Germany, 2020, [Online]. Available: <https://ipg-automotive.com/products-services/simulation-software/carmaker/>
- [43] J. Frey, J. De Schutter, and M. Diehl, "Fast integrators with sensitivity propagation for use in CasADi," 2023.
- [44] R. Verschueren, G. Frison, D. Kouzoupis, J. Frey, N. van Duijkeren, A. Zanelli, B. Novoselnik, T. Albin, R. Quirynen, and M. Diehl, "acados – a modular open-source framework for fast embedded optimal control," *Mathematical Programming Computation*, 2021.
- [45] M. I. I. Sathyamangalam Imran, S. S. Awasthi, M. Khayyat, S. Arrigoni, and F. Braghin, "Virtual validation and uncertainty quantification of an adaptive model predictive controller-based motion planner for autonomous driving systems," *Future Transportation*, vol. 4, no. 4, pp. 1537–1558, 2024, [Online]. Available: <https://www.mdpi.com/2673-7590/4/4/74>
- [46] M. Ester, H.-P. Kriegel, J. Sander, and X. Xu, "A density-based algorithm for discovering clusters in large spatial databases with noise," in *Proceedings of the Second International Conference on Knowledge Discovery and Data Mining*, ser. KDD'96. AAAI Press, 1996, p. 226–231.